Quaternary International 292 (2013) 205–216

Contents lists available at SciVerse ScienceDirect

Quaternary International

journal homepage: www.elsevier.com/locate/quaint

Mineralogical and geochemical studies of glacial sediments from Schirmacher Oasis, East Antarctica

Ashok K. Srivastava [a,*], Kirtikumar R. Randive [b], Neloy Khare [c]

[a] P. G. Department of Geology, SGB Amravati University, Mardi Toad, Amravati, Maharashtra 444 602, India
[b] P. G. Department of Geology, RTM Nagpur University, Nagpur 440 001, India
[c] Ministry of Earth Science, Lodhi Road, New Delhi 110003, India

ARTICLE INFO

Article history:
Available online 27 July 2012

ABSTRACT

Schirmacher Oasis, East Antarctica hosts loose unconsolidated sediments that consist dominantly of sand-silt admixtures with minor clay. These sediments were collected from different glacial environments such as polar ice sheets, inland lakes, exposed bedrock, and coastal shelf areas. Two sediment fractions (coarse 0.25–0.125 mm and fine 0.125–0.063 mm) were separated and chemically analyzed. Mineralogically, the mixture is composed dominantly of quartz and feldspar, and a large variety of heavy minerals: zircon, tourmaline, rutile, garnet, hornblende, hypersthene, enstatite, kyanite, sillimanite, andalusite, zoisite, lawsonite, chlorite, spinel, topaz, and opaques. The clay minerals i.e., chlorite, illite, smectite, kaolinite, and vermiculite constitute a small fraction. There is a mineralogical control over the observed geochemical patterns and anomalies of these sediments. The rare earth element and incompatible trace element spidergrams show relative enrichment in the coarse fraction as against fine fraction, indicating enrichment of the carrier minerals of these elements (mostly heavy minerals) in the coarse fraction. The overall geochemistry of the sediments classifies them as greywacke as per Lindsey, Fe-sand to arenite as per Herron, and sodic sandstones as per Blatt et al. These sediments show quartzose sedimentary provenance, but influence of other unknown sources is also discernible. Transporting agencies for the sediments are commonly meltwater channels and wind. However, transport under influence of gravity, glacier action and sea waves are also envisaged. The sediments have undergone low degrees of chemical weathering ranging between incipient and moderate types.

1. Introduction

Sedimentary rocks contain wealth of information about the composition, tectonic setting, and evolutionary growth of the early continental crusts (Taylor and McLennan, 1985; McLennan et al., 1993). The original composition of weathered source rocks is a dominant control on the makeup of terrigenous sediments, and therefore geographic and stratigraphic variations in provenance can provide important constraints on the tectonic evolution of the region (e.g. Clift et al., 2000; McLennan et al., 2003; Rahman and Suzuki, 2007; Lamaskin et al., 2008). The geochemistry of sedimentary rocks has been used to classify rocks, identify provenance characteristics and investigate palaeoclimatic conditions of depositional basins (e.g. Nesbitt and Young, 1982; Bhatia, 1983; Bhatia and Crook, 1986; Herron, 1988; Armstrong-Altrin and Verma, 2005; Ryan and Williams, 2007). However, little data are available on the geochemistry of the glacial sediments of the study area. This paper characterizes the glacial sediments of the Schirmacher Oasis, East Antarctica on the basis of their mineralogy and geochemistry.

The Schirmacher Oasis comprises high-grade metamorphic terrain (Sengupta, 1986; Singh, 1986) forming the basement, which, at places, hosts loose unconsolidated glacial sediments (Lal, 1986; Asthana and Chaturvedi, 1998). These sediments mainly consist of sand-silt-clay, and have not been studied for their geochemistry. The basement rocks, however, show little attention for their basic geochemical aspects i.e., charnokite and granites (Keshava Prasad and Gaur, 2007) and lamprophyres (Hoch and Tobschall, 1998; Hoch, 1999; Hoch et al., 2001).

The Oasis, in general, is little explored for its geological aspects because of difficult access and limited time for field work. The recent study of grain-size data by Srivastava and Khare (2009) reveals that the sediments of various glacial and geological units exhibit almost similar textural and statistical characteristics as

* Corresponding author.
E-mail address: ashokamt2000@hotmail.com (A.K. Srivastava).

1040-6182/$ – see front matter © 2012 Elsevier Ltd and INQUA. All rights reserved.
http://dx.doi.org/10.1016/j.quaint.2012.07.028

there is an intermixing of the sediments of various units due to ice and wind activities. Therefore, it is necessary to identify the sources of these sediments. The rocky landmass of the Oasis is considered to be the major contributor of sediments. Although very feeble chemical weathering of these rocks is expected in the cold-based environment, some of the rocks show effects of chemical alteration. Considering these aspects, the aims of the present study are to i) interpret the geochemical data (major, minor and trace elements including rare earths), ii) classify the sediments fractions analyzed and to comment on provenance characteristics of the area, and, iii) interpret the degree and pattern of weathering.

2. Geological and glacial features of the area

The Schirmacher Oasis (70° 44′ 30″ S to 70° 46′ 30″ S; 11° 22′ 40″ E to 11° 54′ 00″ E) is an east-west trending narrow strip, ice-free region covering an area of about 35 km^2 (Fig. 1). The maximum width of the Oasis is about 2.7 km in the central part. It has undulating topography consisting of low elevation hills up to 200 m high and depressions formed by glacial valleys and lakes.

Exposed geology is mostly represented by high-grade metamorphic rocks, which form the Precambrian crystalline basement. The major geologic units exposed are i) banded-gneiss, ii) alaskite, iii) garnet-biotite gneiss, iv) calc-gneiss, khondalites and associated migmatites, v) augen-gneiss and vi) streaky-gneiss, which are at places intersected by the dykes of basalt, lamprophyres, pegmatite, dolerite and apatite (Sengupta, 1986) (Fig. 1).

The Oasis region is clearly distinguishable into three units: i) polar ice sheet, ii) Schirmacher mainland including lakes, and iii) coastal-shelf area. All three units extend in east-west directions paralleling the coastline (Fig. 1). The polar ice sheet covers a large area in the south and contains abundant sand and silt-size sediments. The second unit is the exposed rock area. It shows an undulating topography with low altitude hills of 50–200 m and inland lakes formed due to glacier erosion. The northern periphery shows a general steepness towards the coast. Various sub-glacial tills, glacial valleys, and polished bedrock are easily recognizable in this unit. The third unit represented by the coastal region is marked by the presence of coastal sand, which is largely mixed with sediments from inland and the polar ice sheet, transported through meltwater channels.

3. Criteria for sampling and site of collection

The study area is elongated E–W, including the polar ice sheet, exposed rock, lake and adjacent coastal areas. The southern margin of the Oasis is overlain by the polar ice sheet, with the scarp face well exposed south of Maitri base camp (Fig. 2A). This face shows horizontal layering of the ice with distinguishable changes in thickness, shades of brown colors, transparency and degree of melting. The ice-sheet also contains silt and sand which show comparatively higher concentrations in meltwater channels, depressions formed on the surface as well as on the ground where meltwater along with sediments drips down, leaving small debris cones. Southeast wind to 92 knots is also a significant agent (Bera, 2004; Lal and Manchurkar, 2007) which releases the sediments through weathering and erosion followed by their selective deposition in depressions, shadow zones and valleys. The sediments in this area are mainly released by the polar ice due to its melting and dropping of sediments. The exposed rock area (Fig. 2B) includes inland lakes (Fig. 2C, D). On the exposed rock area, both release of sediments and their deposition are considered as result of erosion of basement rocks due to erosional and depositional activities of ice and wind. The lakes are medium to small, freshwater bodies and receive sediments from meltwater discharge (Fig. 2E, F). The third unit in the north grades to the coastal area of the Antarctic Ocean (Fig. 2G). This region is dominantly rocky but sand patches are frequently exposed. Locally, patches of horizontally bedded glacial sediments interlocked in shelf ice are present (Fig. 2H). These three units clearly show variations in their sediment sources, mechanism of transport and deposition. The dominant physical factors controlling the transportation and deposition of these sediments are meltwater channels, wind and ice, also responsible for inter-mixing of the sediments from different units. A total of nineteen sediment samples (A-1 to A-19) were collected from the entire area to represent the geological and glacial units (Fig. 1).

3.1. Polar ice sheet

The polar ice sheet was sampled at surface, margins, and near the base. Four samples were collected around the scarp face, exposed about 500 m south of Maitri:

A-1: Base of polar ice sheet scarp face south of Maitri.
A-2: From the base of polar ice sheet, SW of Maitri.
A-3 and A-4: From the ice sheets lying at the base near the scarp margin at two different locations roughly 500 m apart, south of Maitri.

3.2. Inland lakes and exposed area

Five and four samples were collected from lakes and the exposed Schirmacher mainland area, respectively. In this unit, sampling has been made with two criteria in consideration, i.e., i)

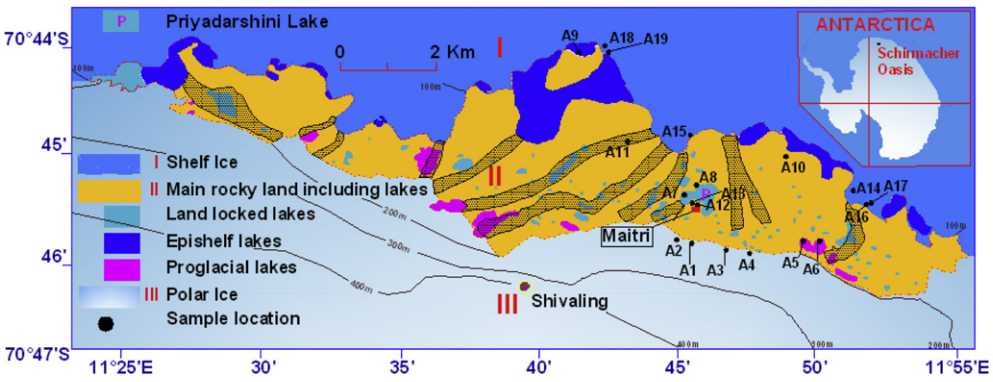

Fig. 1. Map of Schirmacher Oasis showing significant glacial units, elevations, paths of fossil glaciers (after Ravindra, 2001; Gajananda et al., 2007) and locations of sampling sites.

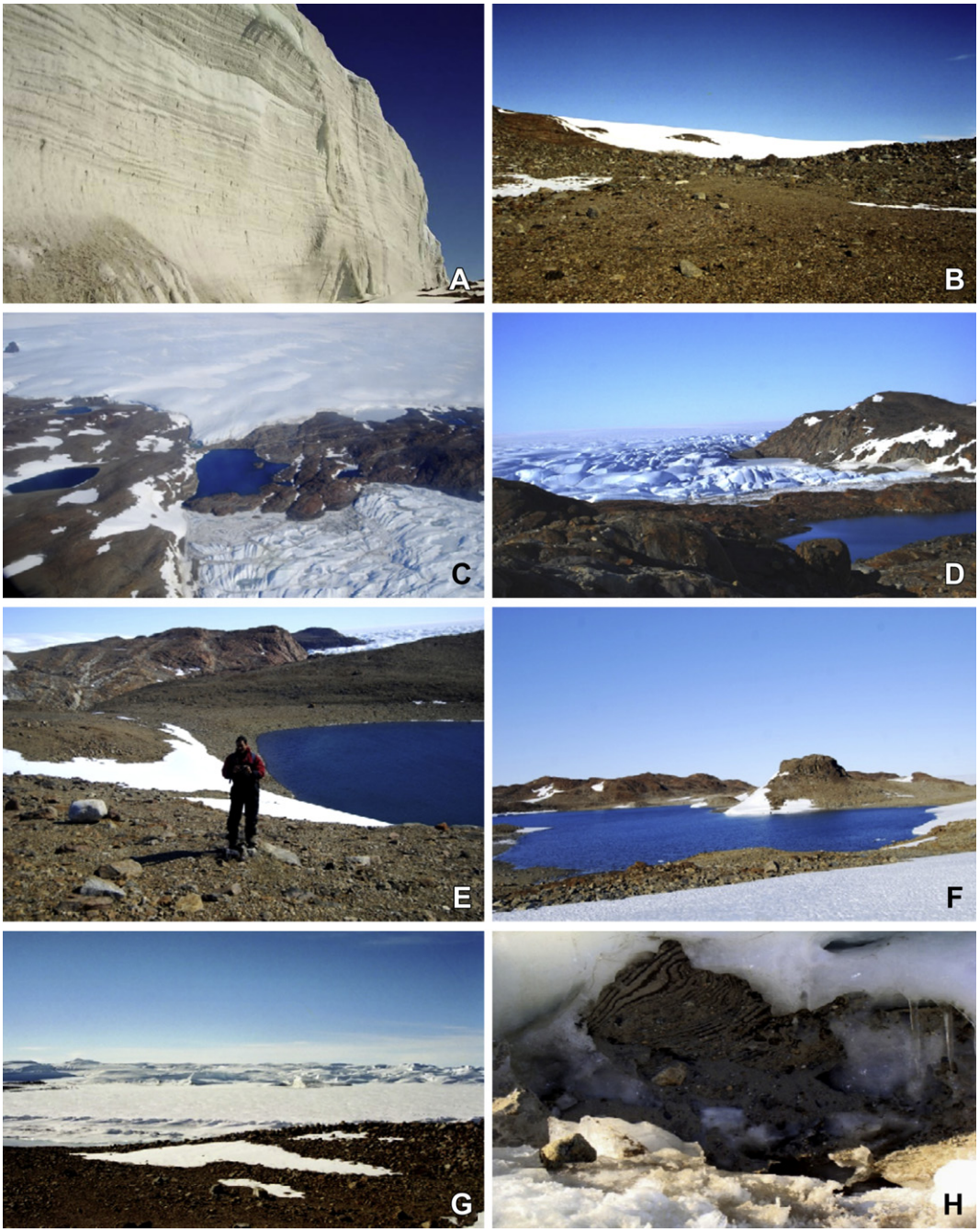

Fig. 2. Photographs showing (A) Scarp face of polar ice sheet exposed in south of Maitri (B) Mainland area showing surface exposure of angular, poorly sorted sediments (C) Aerial view of the lakes near glacier snout. Shivaling Nunatak is seen in the northwest corner, photograph taken from helicopter (D) An inland lake adjacent to the coastline, shelf ice is seen in the background (E) Low lying hills of mainland area including an inland lake (F) Priyadarshini Lake and surrounding mainland area (G) Shelf exposed in the north of Maitri (H) A patch of horizontally bedded glacial sediments interlocked in the shelf ice.

lakes and adjoining area, where meltwater is the main source supplying the sediments, and ii) exposed rocky ground, where wind is a significant factor in sediment accumulation.

A-5: From the lake margin located about 2 km east of Maitri, on the route to Russian station Novalazarevskay.
A-6: Adjacent to A-5.
A-7 and A-8: From the margin of Priyadarshini Lake near Maitri.
A-9: From the margin of epishelf lake located in the extreme north.
A-10: About 2 km NE of Maitri.
A-11: About 2 km NW of Maitri.
A-12 and A-13: From the sand pocket accumulation sites near Maitri at elevations of 2 m and 4 m above the lake, respectively.

3.3. Coastal-shelf area

The northern margin was sampled at four different places, along the roughly E–W trending coastline. A total of six samples have been collected from the coastal-shelf area:

A-14: Shelf 3.5 km east of Maitri.
A-15: From the rocky shelf area, about 3 km west of A-14; north of Maitri.

A-16 and A-17: Two adjacent locations 4 km east of Maitri.
A-18 and A-19: Two locations about 5 km NW of Maitri.

4. Analytical techniques

Two fractions of sediments ranging in size from 0.25 to 0.125 mm and 0.125 to 0.063 mm were separated from the sediments and subjected for chemical analysis. All the major and trace element analyses were carried out at the Wadia Institute of Himalayan Geology, Dehradun, India. The major elements were analyzed using a Siemens SRS 3000 Sequential X-ray Spectrometer with END WINDOW Rh X-Ray Tube following the procedure of Saini et al. (2007). Trace elements were analyzed using a Perkin Elmer SCIEX quadrupole type ICP-Mass Spectrometer ELAN DIRAC-e, adopting the procedure of Khanna et al. (2009). Table 1 shows the analytical data. The samples subjected to chemical analysis have been sieved for grain-size analysis (Srivastava and Khare, 2009), and, heavy minerals separated by gravitational settling method using bromoform (Srivastava et al., 2010). Clay mineral data of the same samples are also available, generated by XRD analysis of Ca and K saturated samples at different temperatures, using a Phillips Analytical X'Pert, Ni-filtered, CuKα radiation with a scanning speed of $2^{\circ}2Ø\ min^{-1}$ (Srivastava et al., 2011).

5. Results and discussion

5.1. Mineralogy

Texturally, the sediments are dominantly medium sand, poorly sorted, near symmetrical to fine-skewed, coarse or fine skewed (Table 2). Each of the sediment samples is enriched in quartz and feldspar. The heavy mineral analysis show that the minerals present in these sediments include zircon, tourmaline, rutile, garnet, hornblende, hypersthenes, enstatite, kyanite, sillimanite, andalusite, zoisite, lawsonite, chlorite, spinel, topaz, and opaques (Srivastava et al., 2010). The X-ray analysis of clay minerals indicates the presence of chlorite, illite, smectite, kaolinite, and vermiculite, apart from quartz and feldspar (Srivastava et al., 2011). The absence of carbonates from the clay mineralogy is significant, as the carbonates often influence source characterization of the sediments. The grain size analysis has shown that there are no significant clay fractions in these sediments (Giordano et al., 1999; Srivastava and Khare, 2009). Table 3 shows total mineralogical estimates of the sediments.

5.2. Geochemistry

Sediments in the size range of 0.25–0.125 mm and 0.125–0.063 mm, separated from the samples collected from the different regions were analyzed (Table 1). The results suggest that the overall SiO_2 content of these sediments ranges between 54.40 and 71.16%. Lower values of SiO_2 were observed for the lake sediments, whereas higher values for the polar ice sheets. Al_2O_3 content varies from 12.72 to 16.11%, with consistently lower values for the polar ice sediments. Total iron content $Fe_2O_3^T$ shows a wider range from 3.84 to 12.72%. However, these values are irregularly distributed between the sediments collected from different regions, but are much lower for the polar ice sediments, which indicate lower degrees of chemical weathering of these sediments. Similarly, MgO content also shows large variation from 1.16 to 7.25%, with relative enrichment in the mainland and lake sediments and depletion in the polar ice sediments. This may indicate that that the ferromagnesian minerals were derived from the exposed rocks that largely contribute sediments to the inland lakes. CaO has a narrow range from 3.22 to 6.22%, with the values almost uniformly distributed within different type of sediments. Na_2O contents are slightly higher for the polar ice sediments with an overall range of 1.71–4.07%. K_2O content ranges from 1.47 to 3.56%, without any preferred enrichment or depletion. TiO_2 content ranges between 0.78 and 2.75%, although these values do not significantly differ in the different sediment types. The overall geochemical characteristics of the sediments from four different glacial environments do not differ significantly, but show some mineralogical control. Chemical analyses of both the size fractions of sediments from four depositional settings were combined in order to study the geochemistry of the glacial sediments of the Schirmacher Oasis.

5.3. Influence of mineralogy on the geochemistry of the sediments

The analyzed fractions (0.25–0.125 mm and 0.125–0.063 mm) do not include the clay mineralogy. Therefore, minerals such as illite, smectite, kaolinite and vermiculite will not represent their influence as the carriers of several major and trace elements by the way of substitution, adsorption or complex formation. However, this should not be a major problem as these sediments are considerably impoverished in clay size sediments (Giordano et al., 1999; Srivastava et al., 2011). Among the other minerals, quartz occurs in overwhelming abundance but it does not influence overall geochemistry, especially trace elements. Similarly, the role of alumino-silicates, namely, andalusite, sillimanite and kyanite as carriers of trace elements is limited, due to the presence of other minerals which are more likely carriers of many major and trace elements. Feldspars are important in this regard since potash feldspars influence Rb, Ba; sodic feldspars Na; and calcic feldspars Sr and Eu. The mafic igneous minerals including hypersthene, enstatite, hornblende and chlorite readily influence the presence of many divalent (Mg^{+2}, Fe^{+2}, Mn^{+2}, Co^{+2}, Cr^{+2}, Ni^{+2}) and some trivalent (Fe^{+3}, Cr^{+3}, Rare Earth Elements (REE^{+3})) elements. Zircon is particularly important as a carrier of majority of the tetravalent elements such as Zr^{+4}, Hf^{+4}, Pb^{+4}, Th^{+4}, Ge^{+4} and U^{+4}. The presence of elements such as B^{+3}, Li^{+}, as well as Na^{+} is influenced by the presence of tourmaline. However, most important mineral is garnet, which is a unique carrier of Heavy Rare Earth Elements (HREE). Similarly, epidote (zoisite) and lawsonite are likely to influence the presence of Middle Rare Earth Elements (MREE), Sr and Eu. In the absence of carbonates; calcic plagioclase and epidote are the leading carriers of Ca (Mason and Moore, 1991; Rollinson, 1993; Ottonello, 1997; Randive, 2012).

The Upper Continental Crust (UCC) normalized REE Patterns (Taylor and McLennan, 1985) of the average coarse (0.25–0.125 mm) and average fine (0.125–0.063 mm) fractions of the sediments of the Schirmacher Oasis are plotted in Fig. 3. The pattern is smooth, showing both curves are mirror images, in which the finer fraction is more depleted compared to the coarse fraction. This may indicate relative impoverishment of the REE carrier minerals such as garnet, epidote and other mafic minerals in the finer fraction. The same trend is observed for other trace elements (Fig. 4). Poor sorting of the glacial sediments may also be one of the reasons. The curves are Light Rare Earth Elements (LREE) depleted shows a negative Eu anomaly and flat HREE; the reason being the absence of LREE carrier mineral phases such as carbonates and apatite in these sediments. Relative impoverishment of plagioclase feldspar as compared to the UCC may account for the negative Eu anomaly, and presence of garnet steadies the HREE contents of these sediments.

The UCC normalized trace element spidergram of the Taylor and McLennan (1985) also shows two curves that are mirror images. However, the overall pattern is Large ion Lithophile Element (LILE) depleted – High Filed Strength Elements (HFSE) enriched with the positive spikes of Th, La, Ce, Hf, Zr and Ti, and negative spikes of Rb, K, Sr and Hf. The heavy minerals, which account for majority of the

Table 1
Chemical analyses of 0.25–0.125 mm and 0.125–0.0625 mm size fractions of the sediments of the Schirmacher Oasis, East Antarctica.

Sample/Major, minor & trace elements		Polar ice-sheet				Lake					Exposed area				Coastal-shelf					
		A1 (i)	A2 (i)	A3 (i)	A4 (i)	A5 (i)	A6 (i)	A7 (i)	A8 (i)	A9 (i)	A10 (i)	A11 (i)	A12 (i)	A13 (i)	A14 (i)	A15 (i)	A16 (i)	A17 (i)	A18 (i)	A19 (i)
0.125 mm																				
Major oxides	SiO_2	60.55	70.31	71.16	66.88	57.97	57.88	61.62	61.88	69.79	60.71	59.68	63.93	59.60	61.25	59.60	64.59	60.33	66.97	54.40
in percentage	TiO_2	2.75	0.93	0.88	1.06	1.90	1.34	1.33	1.49	1.01	1.22	2.06	1.01	1.88	1.67	1.70	1.13	1.73	1.31	1.89
	Al_2O_3	13.79	13.33	12.72	13.17	13.71	14.22	15.50	15.48	13.56	14.97	15.39	15.00	15.49	15.87	14.64	14.45	16.11	13.31	14.69
	Fe_2O_3	9.01	4.62	4.16	5.42	10.27	8.84	6.14	6.58	5.21	7.33	7.53	4.73	7.67	6.76	10.29	4.97	7.32	5.92	11.05
	MgO	3.59	1.19	1.16	1.35	4.03	4.94	3.97	3.90	1.67	4.95	3.54	1.46	3.63	3.94	2.78	1.63	3.96	1.76	6.72
	MnO	0.13	0.08	0.08	0.08	0.13	0.09	0.08	0.09	0.09	0.10	0.11	0.07	0.11	0.11	0.09	0.08	0.11	0.09	0.11
	CaO	5.72	3.68	3.43	3.69	5.12	3.88	4.56	4.66	3.86	4.33	6.22	4.34	6.20	4.88	4.54	4.09	5.36	3.93	4.04
	K_2O	1.83	2.11	2.20	2.22	2.24	3.30	2.37	2.38	1.47	2.73	1.97	2.02	1.90	1.94	1.73	1.88	1.91	1.58	3.00
	Na_2O	3.15	4.07	4.00	3.79	2.77	2.48	3.24	3.30	4.05	2.63	3.36	3.97	3.26	3.27	3.53	3.83	3.34	3.82	2.07
	P_2O_5	0.60	0.46	0.39	0.46	0.94	0.38	0.37	0.44	0.28	0.35	0.78	0.50	0.65	0.36	0.31	0.45	0.48	0.42	0.33
	LOI	0.40	0.80	0.51	0.48	2.24	4.20	1.13	0.96	0.61	1.75	0.63	0.84	0.57	0.72	2.60	0.86	0.89	0.58	2.82
Minor and trace	Ba	719.82	485.84	559.78	448.51	646.40	764.59	662.79	597.02	264.56	624.55	611.89	321.69	590.35	611.05	541.13	350.18	630.43	260.00	605.88
elements in ppm.	Cr	89.84	163.30	145.93	75.14	467.32	527.42	221.56	159.37	240.17	265.86	136.66	179.00	290.65	115.73	351.21	264.23	144.60	109.91	1089.60
	Cu	0.22	12.54	3.60	13.45	17.60	45.03	21.09	21.53	23.95	37.22	9.06	22.47	15.34	19.24	32.70	16.60	27.21	15.73	53.00
	Zn	78.70	70.40	60.47	80.12	162.11	126.38	72.77	68.00	56.86	79.65	76.06	69.46	74.19	67.98	81.14	63.68	77.12	64.95	121.21
	Ga	13.56	13.41	12.45	13.91	16.32	18.32	14.88	14.98	12.82	15.78	14.31	14.14	14.61	14.42	16.18	14.17	14.97	13.49	18.53
	Pb	15.63	15.58	17.52	18.32	16.29	14.99	15.66	14.84	11.10	13.79	15.25	18.79	13.11	15.00	11.03	13.51	14.89	14.65	15.37
	Rb	36.71	49.32	53.68	52.36	53.31	106.43	57.74	56.08	31.76	74.29	41.29	46.42	38.96	43.14	49.54	42.45	42.08	36.10	90.07
	Sr	270.25	290.72	308.50	263.81	210.38	222.74	240.25	227.91	224.13	212.50	263.92	261.20	263.70	242.34	195.32	247.36	244.62	225.15	182.46
	Zr	1120.22	633.83	965.15	586.56	819.73	281.10	362.03	367.35	235.32	349.25	787.44	385.18	572.95	430.97	302.22	489.95	550.99	503.37	329.89
	Nb	26.49	17.63	19.83	18.48	20.93	15.26	12.98	14.07	12.77	14.29	19.15	13.38	17.90	17.23	15.10	16.55	17.25	17.06	15.65
	La	72.83	49.53	87.36	39.92	47.99	54.30	36.01	50.04	25.78	81.08	50.06	32.82	39.76	62.87	53.42	111.45	106.30	34.62	27.89
	Ce	167.97	123.46	191.03	90.93	115.62	115.15	81.11	114.32	57.56	166.33	118.69	74.07	92.99	141.42	122.16	254.21	239.80	76.68	60.38
	Pr	19.50	14.03	21.97	10.86	15.07	13.02	9.60	13.41	7.00	18.18	14.18	8.75	11.20	16.73	14.28	29.88	27.96	9.19	7.28
	Nd	86.01	61.60	94.02	48.99	73.48	55.81	43.18	59.42	31.47	76.11	65.22	40.08	51.41	75.40	64.69	131.74	123.14	41.22	33.50
	Sm	17.56	13.17	17.73	11.56	17.13	11.82	10.05	12.27	7.85	14.63	14.31	9.21	11.37	15.17	12.83	24.59	24.25	10.11	8.58
	Eu	2.28	2.16	1.95	2.19	2.67	2.10	2.20	2.01	1.70	2.11	2.28	1.93	2.07	2.11	2.03	2.66	2.29	2.09	2.02
	Gd	13.79	10.24	13.21	8.42	12.11	8.63	7.55	9.45	6.23	11.49	11.20	7.33	8.62	11.69	9.61	17.86	17.60	8.37	6.19
	Tb	2.36	1.78	2.03	1.59	1.91	1.47	1.40	1.61	1.32	1.81	1.93	1.37	1.54	1.93	1.59	2.73	2.61	1.58	1.22
	Dy	13.23	9.71	10.00	8.65	8.69	7.52	7.94	8.61	8.10	9.27	10.82	8.24	8.80	9.87	8.05	12.99	12.25	9.33	7.03
	Ho	2.68	1.99	1.92	1.82	1.60	1.46	1.60	1.74	1.79	1.80	2.19	1.59	1.74	1.94	1.54	2.45	2.23	2.00	1.46
	Er	7.51	5.76	5.87	5.35	4.62	4.16	4.64	5.09	5.50	5.07	6.38	4.66	4.98	5.48	4.64	7.23	6.25	5.77	4.27
	Tm	1.06	0.83	0.78	0.68	0.52	0.53	0.64	0.76	0.76	0.72	0.94	0.64	0.70	0.75	0.60	0.89	0.88	0.89	0.56
	Yb	6.26	4.82	5.06	4.45	3.41	3.38	4.18	4.50	5.03	4.25	5.63	4.19	4.55	4.64	3.83	5.80	5.32	5.50	3.69
	Lu	0.98	0.73	0.78	0.68	0.53	0.51	0.63	0.68	0.76	0.59	0.86	0.62	0.66	0.68	0.58	0.88	0.82	0.76	0.56
	Sc	20.68	16.74	13.89	17.63	22.31	19.06	17.07	17.38	20.40	18.05	19.23	16.21	18.43	18.59	20.92	17.65	19.66	19.56	21.22
	Y	70.81	55.30	53.69	49.90	43.30	41.20	45.07	49.15	50.20	47.33	61.09	45.81	49.24	51.35	43.36	67.57	60.27	53.75	40.62
	Th	22.07	8.39	36.02	10.77	5.84	9.57	6.09	11.78	6.26	24.04	10.99	6.28	6.82	18.57	15.28	45.32	41.60	7.71	5.12
	V	112.13	87.89	57.49	75.01	95.67	109.51	96.27	89.50	95.89	84.33	89.88	78.75	96.40	89.22	108.13	90.65	96.01	95.85	129.09
	U	3.25	1.86	5.23	2.36	1.60	3.31	1.30	1.26	1.05	2.04	1.39	1.01	1.73	1.72	1.23	6.96	2.54	1.47	1.53
	Hf	12.39	4.21	10.98	3.68	3.22	2.20	4.29	1.95	3.44	2.01	3.49	1.21	4.56	1.82	1.57	17.20	5.26	2.69	1.94
	Co	13.88	10.03	7.64	10.58	19.79	19.87	13.60	12.07	11.31	16.59	12.41	10.59	12.53	11.18	17.32	11.70	14.10	11.86	25.54

(*continued on next page*)

Table 1 (*continued*)

Sample/Major, minor & trace elements		Polar ice-sheet				Lake					Exposed area				Coastal-shelf					
		A1 (ii)	A2 (ii)	A3 (ii)	A4 (ii)	A5 (ii)	A6 (ii)	A7 (ii)	A8 (ii)	A9 (ii)	A10 (ii)	A11 (ii)	A12 (ii)	A13 (ii)	A14 (ii)	A15 (ii)	A16 (ii)	A17 (ii)	A18 (i) i	A19 (ii)
0.0625 mm																				
Major oxides	SiO_2	62.56	67.48	70.08	67.08	55.45	55.62	59.30	58.06	60.95	58.48	59.02	60.18	59.94	61.84	56.73	58.96	59.85	63.01	51.84
in percentage	TiO_2	1.89	0.95	0.78	0.95	1.60	1.36	1.52	1.49	1.90	1.26	2.09	1.44	1.45	1.49	1.49	1.56	1.79	1.61	1.83
	Al_2O_3	14.16	12.93	13.02	13.09	13.87	14.45	15.04	14.96	13.81	14.88	15.46	15.05	15.69	14.31	14.21	15.83	15.49	13.15	14.06
	Fe_2O_3	6.88	4.83	3.84	5.03	11.86	10.20	7.98	9.64	8.43	8.71	7.73	6.97	7.35	7.23	10.24	8.20	7.90	6.84	12.17
	MgO	3.68	1.29	1.17	1.38	3.91	5.31	4.65	4.95	4.79	5.58	3.72	4.19	3.99	4.38	5.76	4.84	4.32	3.17	7.25
	MnO	0.10	0.08	0.07	0.08	0.17	0.09	0.09	0.10	0.12	0.10	0.10	0.09	0.09	0.10	0.08	0.11	0.11	0.10	0.11
	CaO	5.03	3.73	3.54	3.71	4.57	3.22	4.28	4.02	4.94	4.17	5.79	4.95	5.11	4.95	3.95	4.82	5.24	4.12	3.63
	K_2O	2.17	2.20	2.34	2.34	2.65	3.56	2.63	2.96	1.79	3.16	2.19	2.34	2.51	2.13	2.15	2.30	2.04	1.69	3.46
	Na_2O	3.11	3.92	4.01	3.80	2.47	2.18	2.76	2.62	2.82	2.39	3.20	3.15	3.00	2.99	2.60	2.89	3.12	3.56	1.71
	P_2O_5	0.61	0.55	0.44	0.55	1.01	0.34	0.38	0.40	0.43	0.37	0.74	0.54	0.47	0.47	0.32	0.45	0.54	0.46	0.27
	LOI	0.65	0.79	0.80	0.82	4.41	5.31	1.62	2.56	1.01	2.26	0.92	1.04	1.14	1.54	3.29	1.68	1.27	0.82	3.62
Minor and trace	Ba	809.46	564.58	647.12	574.06	770.60	801.47	725.74	677.48	566.05	689.31	717.75	580.63	729.60	729.73	596.23	689.37	674.80	279.19	658.71
elements in ppm.	Cr	272.38	140.99	347.58	282.88	628.49	124.68	159.44	146.77	206.14	585.22	136.17	152.33	105.69	156.51	244.64	583.43	200.41	161.02	253.10
	Cu	24.00	1.29	9.90	9.59	35.67	62.74	24.86	36.38	47.86	45.30	9.68	29.80	69.79	19.90	38.28	33.39	28.78	8.04	71.67
	Zn	108.44	78.84	64.29	82.44	213.73	161.58	98.72	121.77	111.88	101.76	99.29	98.06	137.59	91.02	96.96	107.81	94.87	83.60	154.30
	Ga	12.85	13.06	12.44	13.11	19.27	19.20	16.18	18.66	13.56	15.81	13.95	14.21	15.27	14.43	19.02	16.36	15.61	14.00	20.16
	Pb	17.72	20.16	19.74	18.13	19.79	17.29	15.25	15.86	14.46	16.39	16.55	22.96	17.02	15.52	16.05	13.90	18.05	15.38	14.43
	Rb	47.64	53.85	56.95	57.76	72.92	127.45	71.89	92.91	41.45	88.96	47.87	57.37	61.95	55.62	66.44	59.50	48.50	39.72	111.36
	Sr	293.56	303.09	337.88	289.17	190.90	202.82	222.10	201.57	198.91	199.02	250.48	235.03	240.45	236.05	177.70	228.97	232.90	212.77	167.69
	Zr	1444.07	1104.65	979.80	1024.81	985.25	311.93	538.46	472.65	785.73	402.36	1381.53	709.48	738.23	744.88	415.79	605.78	854.94	1147.99	399.89
	Nb	22.39	20.33	19.29	18.62	17.84	15.41	13.90	14.74	16.99	13.63	20.66	13.96	15.06	17.31	13.79	16.86	17.78	19.96	15.41
	La	38.93	96.91	71.64	75.81	91.05	72.59	67.76	66.38	79.00	72.45	101.97	53.30	48.10	82.76	68.39	90.57	84.73	97.26	62.01
	Ce	87.75	223.01	167.82	176.76	221.36	156.21	149.15	147.71	182.41	160.91	229.08	114.79	103.00	189.19	151.56	199.73	191.27	225.46	138.07
	Pr	10.38	26.88	19.28	20.70	27.73	17.71	17.47	17.08	22.16	18.71	27.64	13.41	11.53	21.85	17.70	23.35	22.82	26.64	16.56
	Nd	46.96	119.86	82.50	89.30	130.50	75.42	78.14	74.56	100.75	81.30	123.26	60.83	54.79	95.73	76.00	103.05	100.44	115.91	71.61
	Sm	10.21	24.71	16.54	18.24	27.93	15.06	15.32	16.10	20.13	16.72	24.04	12.66	8.96	18.12	16.17	20.31	19.59	22.64	13.73
	Eu	2.08	2.88	2.18	2.47	3.27	2.29	2.38	2.75	2.70	2.77	2.67	2.10	1.83	2.37	2.57	2.67	2.63	2.42	2.00
	Gd	8.11	17.91	12.34	13.82	19.18	11.40	10.86	11.78	14.16	12.12	16.96	9.76	7.61	13.44	11.34	14.24	14.38	16.71	10.02
	Tb	1.57	2.85	2.02	2.30	2.51	1.82	1.73	1.98	2.24	1.84	2.63	1.74	1.28	1.99	1.84	2.26	2.18	2.48	1.56
	Dy	8.72	14.81	10.44	12.40	10.79	9.49	9.21	10.57	11.41	9.15	12.58	9.53	6.42	9.92	8.70	10.94	10.74	12.29	8.21
	Ho	1.84	2.79	2.07	2.48	1.84	1.84	1.76	2.04	2.27	1.86	2.40	1.92	1.21	1.95	1.70	2.09	2.14	2.44	1.66
	Er	5.28	8.08	6.04	6.94	5.21	5.43	5.06	5.89	6.51	5.44	7.21	5.63	2.62	5.57	4.95	6.22	6.35	7.16	4.87
	Tm	0.76	1.18	0.85	0.97	0.66	0.74	0.72	0.84	0.93	0.74	0.84	0.81	0.53	0.79	0.62	0.84	0.87	1.02	0.68
	Yb	4.50	7.21	5.18	5.77	4.00	4.40	4.33	4.93	5.70	4.47	5.45	4.72	3.12	4.59	3.88	5.33	5.44	6.29	4.30
	Lu	0.73	1.06	0.78	0.88	0.58	0.66	0.64	0.75	0.87	0.65	0.81	0.70	0.50	0.70	0.58	0.80	0.76	0.97	0.60
	Sc	18.03	20.12	12.87	17.72	24.59	21.52	19.62	22.97	22.01	20.22	18.52	18.49	11.64	20.88	22.95	19.99	19.83	21.48	23.52
	Y	49.77	75.76	56.16	66.75	47.89	48.57	48.40	57.62	59.65	47.36	65.82	52.23	33.39	51.43	46.39	57.85	56.91	64.37	43.18
	Th	8.46	29.11	29.70	23.75	11.16	15.20	16.66	13.64	29.77	17.72	27.92	9.18	12.00	27.56	15.99	27.72	22.45	36.86	22.06
	V	88.08	87.61	60.46	85.96	120.71	114.84	107.53	125.00	128.03	105.89	88.23	85.95	107.00	99.74	119.10	93.72	99.48	112.88	162.67
	U	1.25	5.07	4.88	3.63	2.42	4.65	2.03	2.53	3.38	1.97	3.54	1.84	2.00	2.55	1.75	2.78	2.67	3.47	2.65
	Hf	2.68	5.15	6.40	2.22	5.42	4.19	2.95	5.80	8.58	3.82	8.05	4.71	13.51	5.76	2.94	5.60	8.07	9.02	3.19
	Co	11.37	11.76	7.45	11.15	28.57	23.23	17.79	21.19	15.68	21.19	12.90	13.83	4.04	15.16	20.42	14.99	15.46	13.76	31.07

Table 2
Textural parameters of the samples, trends of average percentages of heavy minerals and clay minerals belonging to different glacial units of the Oasis; (abbreviations used for heavy minerals: Zr – Zircon, Tr – Tourmaline, Rt – Rutile, Gr – Garnet, Hr – Hornblende, Hp – Hypersthene, En – Enstatite, Ky – Kyanite, Si – Sillimanite, An – Andalusite, Zo – Zoisite, La – Lawsonite, Ch – Chlorite, Sp – Spinel, To – Topaz, Op – Opaque; for clay minerals: Ch – Chlorite, Il – Illite, Ka – Kaoline, Sm – Smectite, Ve – Vermiculite).

Glacial units	Sample number	Textural parameters				Average percentage (*X*-axix) of heavy minerals	Average percentage (*X*-axix) of clay minerals in clay fractions
		Mean (M_Z)	Standard deviation (σ_1)	Skewness (Sk_1)	Kurtosis (K_G)		
Polar ice-sheet	A-1	Medium sand; 1.24	Poorly sorted; 1.88	Fine-skewed; +0.21	Mesokurtic; 1.10		
	A-2	Medium sand; 1.29	Poorly sorted; 1.81	Fine-skewed; +0.14	Mesokurtic; 0.98		
	A-3	Coarse sand; 0.98	Very poorly sorted; 2.08	Very fine-skewed; +0.40	Very platykurtic; 0.62		
	A-4	Coarse sand; 0.93	Poorly sorted; 1.98	Nearly-symmetrical; 0.05	Platykurtic; 0.71		
Lake	A-5	Medium sand; 1.18	Poorly sorted; 1.81	Fine-skewed; +0.13	Platykurtic; 0.73		
	A-6	Coarse sand; 0.47	Poorly sorted; 1.75	Nearly-symmetrical; +0.09	Platykurtic; 0.77		
	A-7	Medium sand; 1.23	Very poorly sorted; 2.19	Very fine-skewed; +0.26	Platykurtic; 0.71		
	A-8	Medium sand; 1.11	Very poorly sorted; 2.04	Very fine-skewed; +0.33	Platykurtic; 0.70		
Exposed area	A-9	Medium sand; 1.28	Poorly sorted; 1.50	Fine-skewed; +0.25	Mesokurtic; 0.94		
	A-10	Coarse sand; 0.89	Very poorly sorted; 2.25	Nearly-symmetrical; +0.10	Platykurtic; 0.83		
	A-11	Fine sand; 2.07	Poorly sorted; 1.52	Fine-skewed; +0.25	Very leptokurtic; 1.70		
	A-12	Medium sand; 1.59	Moderately sorted; 0.89	Nearly-symmetrical; −0.01	Leptokurtic; 1.12		
	A-13	Fine sand; 2.18	Poorly sorted; 1.59	Very fine-skewed; +0.37	Mesokurtic; 0.96		
Coastal-shelf	A-14	Medium sand; 1.61	Poorly sorted; 1.53	Nearly-symmetrical; +0.07	Leptokurtic; 1.13		
	A-15	Medium sand; 1.31	Very poorly sorted; 2.08	Nearly-symmetrical; −0.06	Platykurtic; 0.83		
	A-16	Medium sand; 1.78	Poorly sorted; 1.75	Fine-skewed; +0.22	Mesokurtic; 1.05		
	A-17	Medium sand; 1.11	Poorly sorted; 1.91	Very fine-skewed; +0.37	Very leptokurtic; 2.02		
	A-18	Medium sand; 1.27	Poorly sorted; 1.92	Fine-skewed; +0.30	Platykurtic; 0.88		
	A-19	Coarse sand; 0.91	Poorly sorted; 1.66	Nearly-symmetrical; +0.03	Platykurtic; 0.86		

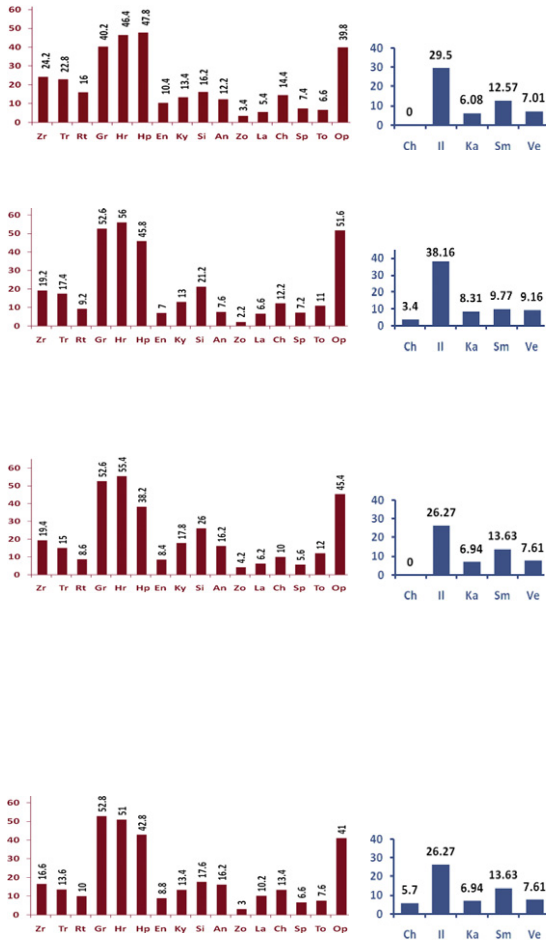

compatible trace elements (HFSE), are responsible for the pattern of the spidergram. Positive spikes of Th, Zr and Ti can be ascribed to the presence of minerals such as zircon and anatase/rutile. Similarly, negative spikes of Rb, K and Sr might be ascribed to the relative depletion of feldspars in these sediments as compared to the UCC.

5.4. Classification

Unlike many igneous rocks, it is difficult to find a simple relationship between the mineralogy of sandstones and their chemical composition. For this reason, the geochemical classification of sandstones does not mimic the conventional mineralogical classification of sandstones based upon quartz-feldspar-lithic fragments. Rather, it differentiates between mature and immature sediments (Rollinson, 1993). The glacial sediments of the Schirmacher Oasis yield interesting results of their geochemical analysis. The log (K_2O/Na_2O) vs log (SiO_2/Al_2O_3) diagram after Lindsey (1999) plots the majority of the data in the greywacke field (Fig. 5). The Log (SiO_2/Al_2O_3) vs log ($Fe_2O_3^T$/K_2O) diagram of Herron (1988) distributes the data points between Fe-sand, wacke and litharenite (Fig. 6). Similarly, the triangular Na_2O–($Fe_2O_3^T$ + MgO)–K_2O diagram of Blatt et al. (1972) indicates that the majority of the data points represents sodic sandstones and the remaining ferromagnesian potassic sandstones (Fig. 7).

5.5. Provenance characteristics

Characterizing the glacial sediments could be difficult due to non-uniformity of the sediments as well as possibility of the windborne sediments being mixed with them. Earlier studies (Srivastava and Khare, 2009) suggested that the glacial sediments of the Schirmacher Oasis collected from different sites (polar ice sheets, mainland, lakes and shelf area) are fairly uniform, dominated by the medium size sand fraction with an average value of 1.47Φ.

Table 3
Total mineralogical estimate of the sediments from different glacial environments of the Schirmacher Oasis, East Antarctica. Minerals are listed in the order of their decreasing abundance (Refer Srivastava and Khare, 2009; Srivastava et al., 2010, 2011, for actual estimates).

Sr. No.	Type of analysis	Particle size	Polar ice-sheet	Inland lakes	Exposed area	Coastal-shelf
1.	Visual estimate and microscopy	Granule Very coarse sand Coarse sand	← Quartz and Feldspar →			
2.	Heavy mineral analysis	Medium sand Fine sand	Hypersthene Hornblende Garnet Zircon Tourmaline Sillimanite Rutile Chlorite Kyanite Andalusite Enstatite Spinel Topaz Lawsonite Zoisite	Hornblende Garnet Hypersthene Sillimanite Zircon Tourmaline Kyanite Chlorite Topaz Rutile Andalusite Spinel Enstatite Lawsonite Zoisite	Hornblende Garnet Hypersthene Sillimanite Zircon Kyanite Andalusite Tourmaline Topaz Chlorite Rutile Enstatite Lawsonite Spinel Zoisite	Hornblende Garnet Hypersthene Sillimanite Zircon Tourmaline Kyanite Rutile Andalusite Chlorite Topaz Enstatite Lawsonite Spinel Zoisite
3.	XRD/DT/TG analyses	Fine silt and clay	Illite Amphibole Ca-Feldspar Smectite K-Feldspar Vermiculite Quartz Kaolinite	Illite Amphibole K-Feldspar Smectite Vermiculite Kaolinite Quartz Ca-Feldspar Chlorite	Illite K-Feldspar Smectite Amphibole Quartz Vermiculite Kaolinite Ca-Feldspar Chlorite	Illite Smectite Amphibole K-Feldspar Vermiculite Kaolinite Quartz Chlorite

Therefore, the geochemical characters of these sediments are uniform and can be used for provenance studies. The wind-borne sediments occupy all the studied regions, and show little compositional deviation from the normal range, and may also be used for the provenance studies.

The diagrams based on the discriminant functions used by Roser and Korsch (1988) are useful. The discriminant functions (DF-1 and DF-2) in first diagram (Fig. 8) are calculated using the following formulae:

$$\text{D.F.1} = -1.773\ TiO_2 + 0.607\ Al_2O_3 + 0.76\ Fe_2O_3^{Total} - 1.5\ MgO + 0.616\ CaO + 0.509\ Na_2O - 1.224\ K_2O - 9.09$$

$$\text{D.F.2} = 0.445\ TiO_2 + 0.07\ Al_2O_3 - 0.25\ Fe_2O_3^{Total} - 1.142\ MgO + 0.438\ CaO + 1.475\ Na_2O - 1.426\ K_2O - 6.861$$

In this diagram, the majority of the data points are plotted in the field of quartzose sedimentary provenance.

The sediments collected from Schirmacher Oasis mostly come from three different sources: i) the glacial sediments derived from the exposed rock area which are composed of metamorphic basement and igneous intrusions and have very short transport distances; ii) wind-borne sediments which could have mixed source regions and very long transport; and iii) beach sediments

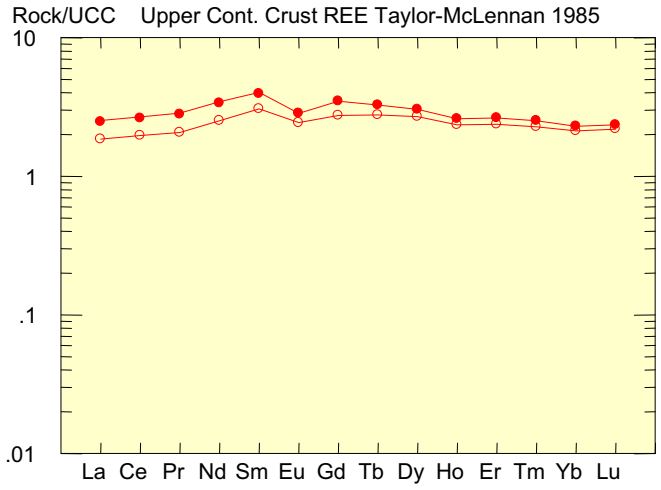

Fig. 3. The Upper Continental Crust normalized REE pattern of the sediments of the Schirmacher Oasis. Filled circles – coarse sediment (0.125 mm), empty circles – fine sediment (0.063 mm) fractions.

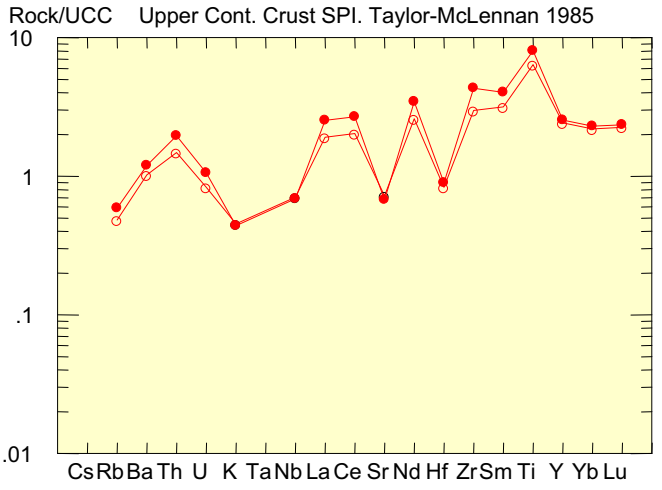

Fig. 4. The Upper Continental Crust normalized trace element spidergrams of the sediments of the Schirmacher Oasis. Filled circles – coarse sediment (0.125 mm), empty circles – fine sediment (0.063 mm) fractions.

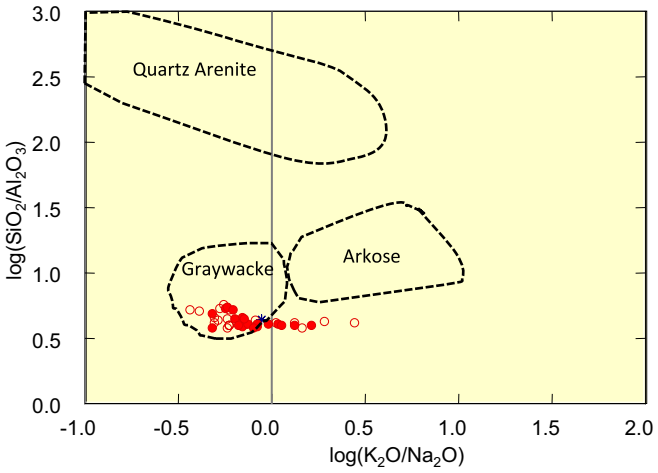

Fig. 5. Log(K_2O/Na_2O) vs log(SiO_2/Al_2O_3) diagram after Lindsey (1999) showing fields for the sandstones.

which could involve long transport and varied sources. Sample locations (glacial environments), their possible sources and possible contaminations from other sources are given in Table 4. This data indicates that the collected sediments belong to different environments, but are mostly derived from the metamorphic basement and intrusive igneous rocks. The influence of other sources is also a governing factor. Although it is very difficult to estimate the provenance of wind-borne and wave-borne sediments, geochemical data provides fairly good estimates.

The sediments belonging to different glaciological environments show reasonably good segregation of data points. Fig. 9 plots variation of CaO against SiO_2, wherein the mainland sediments show relatively higher CaO whereas inland lakes follow the trend of low CaO – low SiO_2. This indicates that the lacustrine sediments are high-density, sufficiently enriched in heavy minerals and transported by surface meltwater channels. On the other hand there are low density, low CaO – high SiO_2, dominantly quartzo-feldspathic sediments, which are in all probability wind-borne. The sediments from the coastal shelf show a scatter of data points, indicating mixed sources of meltwater channels, wind and waves.

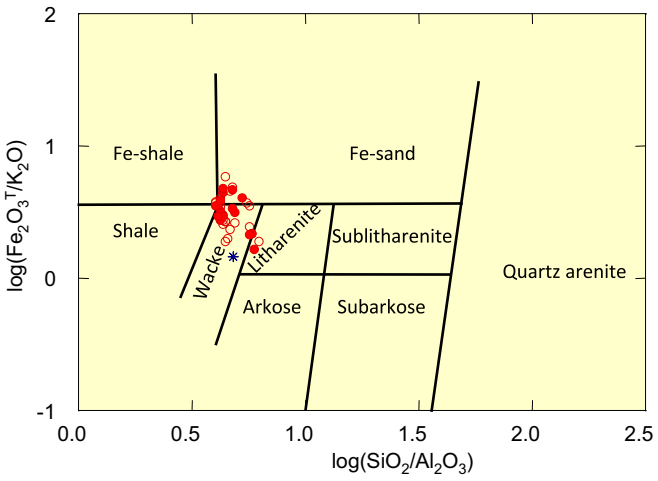

Fig. 6. Log(SiO_2/Al_2O_3) vs log($Fe_2O_3^T/K_2O$) (diagram after Herron (1988) showing plot for the sediments of Schirmacher Oasis.

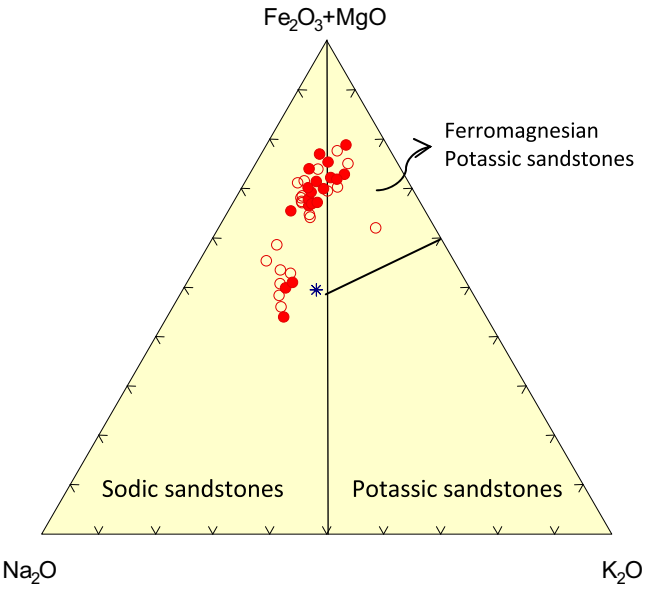

Fig. 7. Triangular scattergram of Na_2O–K_2O–($Fe_2O_3^T$ + MgO) from Blatt et al. (1972) showing the data points of Schirmacher Oasis.

Fig. 10 shows variation of SiO_2 vs MgO + FeO, where all the data points fall along a straight line having negative slope and high correlation coefficient ($r = 0.95$ and r' = 0.94). The majority of the mainland sediments occupy a small circular area indicating that these were derived from the country rocks and lack substantial transport. The sediments collected from inland lakes surround mainland sediments and indicate shorter transport by ice and gravity. The mainland and lake sediments are surrounded by an elongated elliptical area comprising shelf sediments, indicating mixed sources for these sediments. The polar ice sediments form a separate domain. These low density quartzo-feldspathic sediments are considered to be wind-borne. Some of the data from each environment fall towards the polar ice domain. The wind-borne sediments may occupy mainland, lake, and coastal shelf areas.

The separate influence of meltwater and wind transport on the geochemistry of sediments of Schirmacher Oasis is shown in the

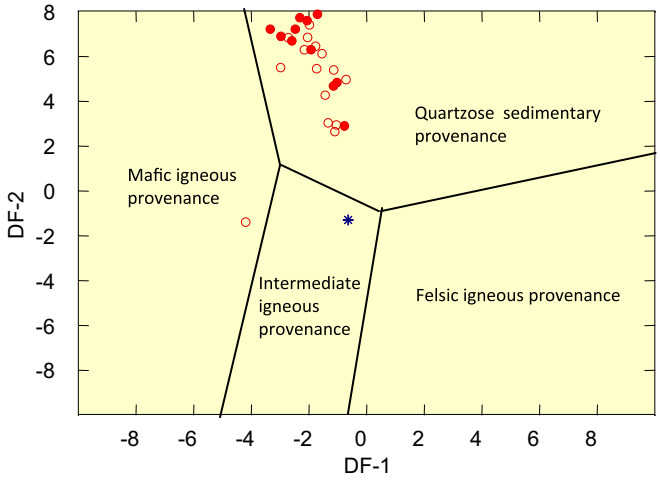

Fig. 8. The provenance discrimination diagrams after Roser and Korsch (1988) showing the data points in the field of the quartzose sedimentary provenance. See text for the formulae for discriminant functions DF-1 and DF-2 for each diagram.

Table 4
Possible sources and agencies of transport for the sediments of Schirmacher Oasis, East Antarctica.

Sr. No.	Sediment environment	Expected agencies of transport and deposition	Expected source of sediments	Expected length and duration of transport
1.	Polar ice-sheet	Wind	Mainland Antarctic region and surrounding continental areas (depending upon direction and velocity of wind)	Long distance, possibly longer duration
2.	Inland lakes	Meltwater channels + down slope movement of the sediments from surrounding highland	Mainland of Schirmacher Oasis	Short distance, mixed duration
3.	Exposed area	Meltwater channels + wind (mainland rocks obstructing wind)	Mainland rocks and unknown sources	Mixed (long and short) distance and duration
4.	Coastal shelf area	Sea waves + meltwater channels + wind	Coastal Antarctic region + mainland + unknown sources of wind	Mixed (expected to be highly variable)

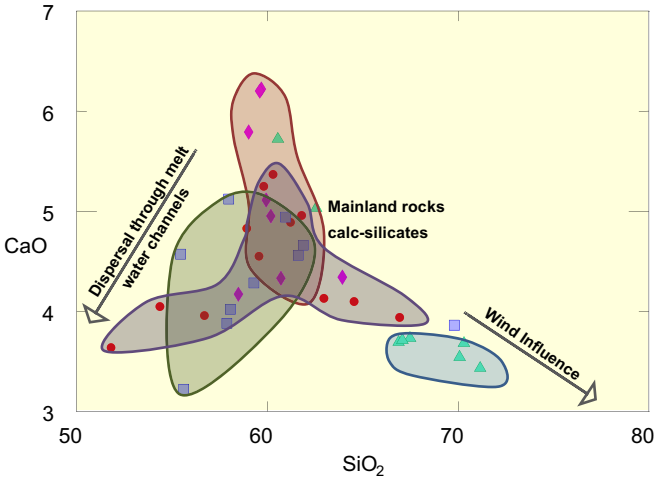

Fig. 9. SiO_2 vs CaO diagram showing trends and possible sources of sediments of Schirmacher Oasis. The symbols used in the diagram indicate sediments collected from different glaciological environments: Diamonds – Mainland, Squares – Lakes, Circles – Coastal Shelf, and Triangles – Polar Ice. See text for discussion.

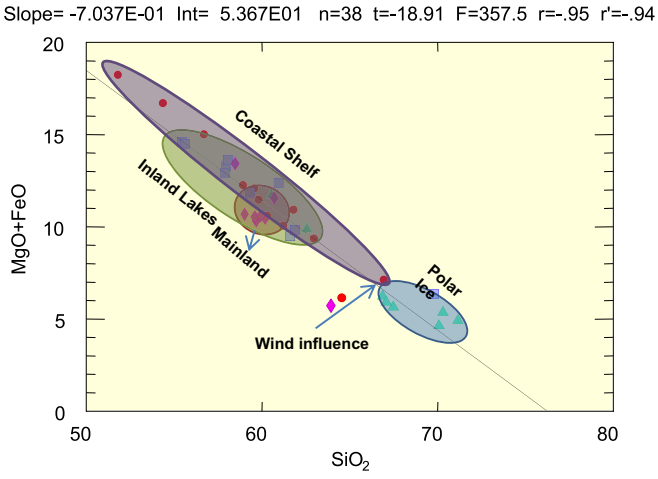

Fig. 10. SiO_2 vs MgO + FeO diagram showing trends and possible sources of sediments of Schirmacher Oasis. Sediments collected all environments fall on a straight line indicating good correlation among the parameters used. The mainland sediments occupy a smaller area, which is completely overlapped by the sediments from inland lakes and both areas by the sediments from coastal shelf. The polar ice sediments fall on the same line but out of these influences. Symbols as per Fig. 9.

$Na_2O + K_2O$–CaO–MgO + FeO diagram (Fig. 11). In this diagram, a small circular area is occupied by mainland sediments, whereas Trend 1 shows influence of wind and Trend 2 shows influence of meltwater transport. Thus, the sediments collected from four different glaciological environments have different sources as depicted in Table 3.

5.6. Evaluation of chemical weathering

Chemical weathering can influence the major element geochemistry of the sedimentary rocks, most significantly by the alteration of feldspars and volcanic glass (Nesbitt and Young, 1982; Taylor and McLennan, 1985). The degree of chemical weathering can be evaluated using the Chemical Index of Alteration (CIA) proposed by Nesbitt and Young (1982) as stated below:

$$CIA = Al_2O_3/\left(Al_2O_3 + K_2O + Na_2O + CaO^*\right) \times 100,$$

where, CaO* represents CaO in silicates (Nesbitt and Young, 1989; Nesbitt et al., 1996). A CIA value of 100 indicates intense chemical weathering along with complete removal of all alkali and alkaline earth elements, whereas CIA values of 45–55 indicate virtually no weathering. Almost all the sediments of Schirmacher Oasis show

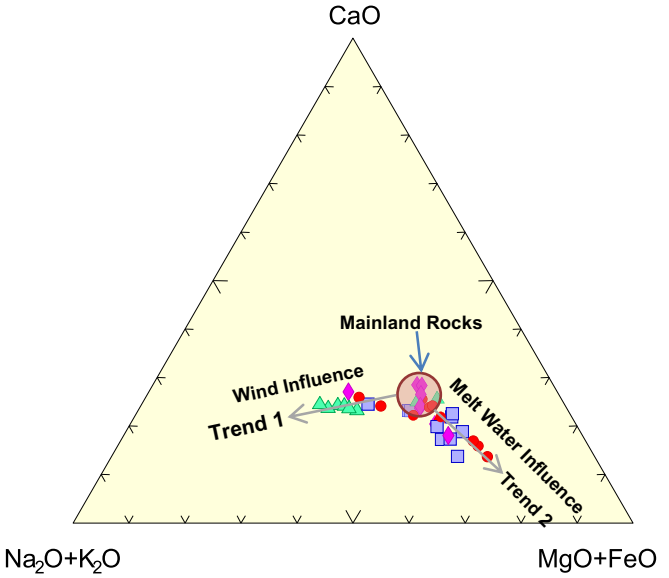

Fig. 11. $Na_2O + K_2O$–CaO–MgO + FeO diagram showing weathering trends, possible source rocks vis-a-vis sediments from Schirmacher Oasis. The circle in the middle shows sediments from mainland. Trend 1 shows data points for the wind-borne sediments; whereas Trend 2 shows sediments transported by melt-water channel. Symbols as per Fig. 9.

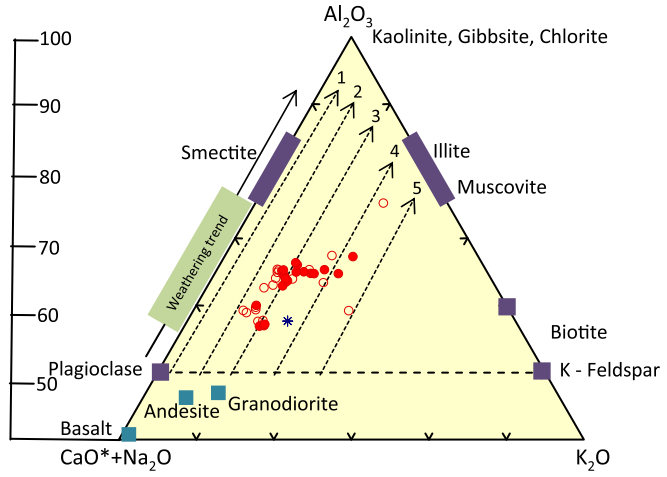

Fig. 12. A–CN–K diagram showing weathering trends, possible source rocks vis-avis sediments from Schirmacher Oasis. Weathering are 1. Gabbro, 2. Tonalite, 3. Diorite, 4. Granodiorite, 5. Granite. The diagram and trends after Nesbitt and Young (1982), Rashid (2002) and Lamaskin et al. (2008).

values ranging between 56 and 66, which means that these sediments are juvenile and relatively immature. There is an Index of Compositional Variability (ICV), which can also be used to discriminate source rock types based on major element geochemistry (Cox et al., 1995; Potter et al., 2005), where,

$$\mathrm{ICV} = \left(\mathrm{CaO} + \mathrm{K_2O} + \mathrm{Na_2O} + \mathrm{Fe_2O_3^T} + \mathrm{MgO} + \mathrm{TiO_2}\right) \Big/ \mathrm{Al_2O_3}$$

A high ICV value indicates compositionally immature source rocks rich in non-clay silicate minerals, whereas low values represent compositionally mature source rocks. Therefore, as weathering progresses, ICV values decreases due to conversion of feldspars to Al-bearing clays. The ICV values for the sediments of Schirmacher Oasis range between 2.1 and 1.2 and indicate an immature source rock undergoing progressive weathering.

The ternary plot of the Chemical Index of Alteration (CIA) and Al_2O_3–($CaO^* + Na_2O$)–K_2O (ACNK) after Nesbitt and Young (1982) shows a degree of source rock weathering (Fig. 12). This weathering trend on this diagram suggests that the glacial sediments have experienced incipient to moderate chemical weathering.

It is not surprising that the data shows low degrees of weathering, especially in a cold-based glacial environment. Nevertheless, in a few horizons, the country rocks show imprints of weathering which may be a representative of pre-glacial tropical-subtropical climatic conditions. Although the clay fraction is not represented in the chemical analysis, its overall content is very low (Srivastava et al., 2011). Therefore, the degree of weathering can at the most range between incipient to low to moderate. This clearly means that the sediments collected from Schirmacher Oasis are relatively young.

6. Conclusions

The mineralogical and geochemical study of the glacial sediments of the Schirmacher Oasis has indicated that, although there are smaller differences amongst the sediments collected from different regions such as polar ice, inland lakes, mainland and shelf areas, they altogether represent similar geochemical characteristics. Mineralogy, especially heavy minerals, has a considerable influence on the geochemical patterns and anomalies observed in these sediments. The important conclusions from this study are as follows:

(a) The analyzed sediment fractions can be variously classified as greywacke, Fe-sand and sodic sandstones using separate schemes of classification.
(b) The sediments are most probably derived from the quartzose sedimentary provenance.
(c) The sediments were transported by meltwater channels, wind and other sources such as transport by gravity, waves and glaciers.
(d) These sediments have experienced low degrees, incipient to moderate, of chemical weathering.

Acknowledgements

The work has been carried out under the financial assistance of Council of Scientific and Industrial Research, Government of India, New Delhi, provided to AKS in the form of a major research project, No. 24/287/16, EMR-II. The samples were collected by AKS during 21st Indian Scientific Expedition to Antarctica. AKS and KRR thank National Centre for Antarctic and Ocean Research (NCAOR), Goa for providing financial and logistic assistance during 21st and 31st Indian Scientific Expedition to Antarctica respectively. AKS acknowledges the cooperation extended by Sri R.P. Lal, Leader of the expedition, Sri M.P. Gaur, Sri A.V. Keshava Prasad and Dr. N. Sharma; whereas, KRR gratefully acknowledges support provided by Dr. Rasik Ravindra, Shri. Uttam Chand, Dr. Rajesh Asthana, Dr. Javed Baig, Dr. Rahul Mohan and Dr. Shailesh Saini. Analytical work was carried out at Wadia Institute of Himalayan Geology, Dehradun under the supervisions of Dr. P.P. Khanna and Dr. N.K. Saini.

References

Armstrong-Altrin, J.S., Verma, S.P., 2005. Critical evaluation of six tectonic setting discrimination diagrams using geochemical data of Neogene sediments from known tectonic settings. Sedimentary Geology 177, 115–129.
Asthana, R., Chaturvedi, A., 1998. The grain size behavior and morphoscopy of supraglacial sediments, south of Schirmacher Oasis, E. Antarctica. Journal of the Geological Society of India 52, 557–568.
Bera, S.K., 2004. Late Holocene palaeo-winds and climatic changes in Eastern Antarctica as indicated by long-distance transported pollen-spores and local microbiota in polar lake core sediments. Current Science 86 (11), 1485–1488.
Bhatia, M.R., 1983. Plate tectonics and geochemical composition of sandstones. Journal of Geology 91, 611–627.
Bhatia, M.R., Crook, A.W., 1986. Trace element characteristics of graywackes and tectonic setting discrimination of sedimentary basins. Contributions to Mineralogy and Petrology 92, 181–193.
Blatt, H., Middleton, G., Murray, R., 1972. Origin of Sedimentary Rocks: Englewood Cliffs. Prentice Hall, New Jersey, 634 pp.
Clift, P.D., Degnan, P.J., Hannigan, R., Blusztajn, J., 2000. Sedimentary and geochemical evolution of the Dras forearc basin, Indus suture, Ladakh Himalaya, India. Geological Society of America Bulletin 112, 450–466.
Cox, R., Lowe, D.R., Cullers, R.L., 1995. The influence of sediment recycling and basement composition of evolution of mudrock geochemistry in southwestern United States. Geochimica et Cosmochimica Acta 59, 2919–2940.
Gajananda, K., Dutta, H.N., Lagun, V.E., 2007. An episode of coastal advection fog over East Antarctica. Current Science 93 (5), 654–659.
Giordano, R., Lombardi, G., Ciaralli, L., Beccaloni, E., Sepe, A., Ciprotti, M., Costantini, S., 1999. Major and trace elements in sediments from Terra Nova Bay, Antarctica. The Science of the Total Environment 227, 29–40.
Herron, M.M., 1988. Geochemical classification of terrigenous sands and shales from core or log data. Journal of Sedimentary Petrology 58 (5), 820–829.
Hoch, M., 1999. Geochemistry and petrology of ultramafic lamprophyres from Schirmacher Oasis, East Antarctica. Mineralogy and Petrology 65, 51–67.
Hoch, M., Tobschall, H.J., 1998. Minettes from Schirmacher Oasis, East Antarctica – indicators of an enriched mantle source. Antarctic Science 10 (4), 476–486.
Hoch, M., Rehkamper, M., Tobschall, H.J., 2001. Sr, Nd, Pb and O Isotopes of minettes from Schirmacher Oasis, East Antarctica: a case of mantle metasomatism involving subducted continental material. Journal of Petrology 42 (7), 1387–1400.
Keshava Prasad, A.V., Gaur, M.P., 2007. Geological Mapping of Muhlig-hofmann Mountains, Cdml, East Antarctica. In: 21st Indian Science Expedition to Antarctica. Ministry of Earth Sciences, Technical Publication No. 19, pp. 155–171.
Khanna, P.P., Saini, N.K., Mukherjee, P.K., Purohit, K.K., 2009. An appraisal of ICP-MS technique for determination of REEs: long term QC assessment of silicate rock analysis. Himalayan Geology 30 (1), 95–99.

Lal, M., 1986. Sedimentology of the Glacial Sands and Lake Terraces Sediments from Schirmacher Oasis and Sea Bed Sediment of Princess Astrid Coast, Queen Maud Land, Antarctica. Scientific Report of the 3rd Indian Science Expedition to Antarctica. DOD, Government of India Publication, Technical Publication No. 3, pp. 219–223.

Lal, R.P., Manchurkar, P., 2007. Study of Meteorological Parameters and Ozone Hole Phenomena at Schirmacher Oasis, Antarctica During 21st Indian Expedition 2002–2003. Scientific Report, 21st Indian Scientific Expedition to Antarctica. Department of Ocean Development, Government of India, Technical Publication No. 19, pp. 73–93.

Lamaskin, T.A., Dorsey, B.J., Vervoort, J.D., 2008. Tectonic controls on mudrock geochemistry, Mesozoic rocks of eastern Oregon and Western Idaho, U.S.A.: implications for Cordilleran tectonics. Journal of Sedimentary Research 78, 765–783.

Lindsey, D.A., 1999. An Evaluation of Alternative Chemical Classification of Sandstones. United States Geological Survey Open-file Report 99–346 Electronic Edition, Denver, Colorado, 23 pp.

Mason, B., Moore, C.B., 1991. Principles of Geochemistry. John Wiley and Sons Inc., New Delhi, Second Wiley Eastern Reprint, 350 pp.

McLennan, S.M., Hemming, S., McDaniel, D.K., Hansen, G.N., 1993. Geochemical approaches to sedimentation, provenance and tectonics. In: Johansen, M.J., Basu, A. (Eds.), Processes Controlling the Composition of Clastic Sediments. Geological Society of America, Special Paper 284, pp. 21–40.

McLennan, S.M., Bock, B., Hemming, S.R., Hurrowitz, J.A., Lev, S.M., McDaniel, D.K., 2003. The roles of provenance and sedimentary processes in the geochemistry of sedimentary rocks. In: Lentz, D.R. (Ed.), Geochemistry of Sediments and Sedimentary Rocks: Evolutionary Considerations to Mineral-deposit Forming Environments. Geological Association of Canada, Geotext, vol. 4, pp. 7–38.

Nesbitt, H.W., Young, G.M., 1982. Early Proterozoic climates and plate motions inferred from major element chemistry of lutites. Nature 229, 715–717.

Nesbitt, H.W., Young, G.M., 1989. Formation and diagenesis of weathering profiles. Journal of Geology 97, 129–147.

Nesbitt, H.W., Young, G.M., McLennan, S.M., Keays, R.R., 1996. Effects of chemical weathering and sorting on the petrogenesis of siliciclastic sediments implications for provenance studies. Journal of Geology 104, 525–542.

Ottonello, G., 1997. Principles of Geochemistry. Columbia University Press, New York, 894 pp.

Potter, P.E., Maynard, J.B., Depetris, P.J., 2005. Mud and Mudstones: Introduction and Overview. Spinger-Verlag, Heidelberg. 297 p.

Rahman, M.J.J., Suzuki, S., 2007. Geochemistry of sandstones from the Miocene Surma Group, Bengal basin, Bangladesh: implications for provenance, tectonic setting and weathering. Geochemical Journal 41, 415–428.

Randive, K.R., 2012. Elements of Geochemistry, Geochemical Exploration and Medical Geology. Research Publishing Services, Singapore, 454 p.

Rashid, S.A., 2002. Geochemical characteristics of Mesoproterozoic clastic sedimentary rocks from the Chakrata formation, lesser Himalaya: implications for crustal evolution and weathering history in the Himalaya. Journal of Asian Earth Sciences 21, 283–293.

Ravindra, R., 2001. Geomorphology of Schirmacher Oasis, East Antarctica. In: Geological Survey of India, Special Publication 53, pp. 379–390.

Rollinson, H.R., 1993. Using Geochemical Data: Evaluation, Presentation, Interpretation. Longman Scientific and Technical, England, U. K, 352 pp.

Roser, B.P., Korsch, R.J., 1988. Provenance signatures of sandstone – mudstone suites determined using discrimination function analysis of major-element data. Chemical Geology 67, 119–139.

Ryan, K.M., Williams, D.M., 2007. Testing the reliability of discrimination diagrams for determining the tectonic depositional environment of ancient sedimentary basins. Chemical Geology 242, 103–125.

Saini, N.K., Mukherjee, P.K., Khanna, P.P., Purohit, K.K., 2007. A proposed amphibolites reference rock sample (AM-H) from Himachal Pradesh. Journal of the Geological Society of India 69 (4), 799–802.

Sengupta, S.M., 1986. Geology of Schirmacher Range (Dakshin Gangotri), East Antarctica. Scientific Report of the 3rd Indian Science Expedition to Antarctica. DOD, Government of India Publication, Technical Publication No. 3, pp. 187–217.

Singh, R.K., 1986. Geology of Dakshin Gangotri Hill Range, Antarctica. Scientific Report of the 3rd Indian Science Expedition to Antarctica. DOD, Government of India Publication, Technical Publication No. 3, pp. 181–186.

Srivastava, A.K., Khare, N., 2009. Granulometric analysis of glacial sediments, Schirmacher Oasis, East Antarctica. Journal of the Geological Society of India 73, 609–620.

Srivastava, A.K., Khare, N., Ingle, P.S., 2010. Textural characteristics, distribution pattern and provenance of heavy minerals in glacial sediments of Schirmacher Oasis. East Antarctica Journal of the Geological Society of India 75, 393–402.

Srivastava, A.K., Khare, N., Ingle, P.S., 2011. Characterization of clay minerals in the sediments of Schirmacher Oasis, East Antarctica: their origin and climatological implications. Current Science 100 (3), 363–372.

Taylor, S.R., McLennan, S.M., 1985. The Continental Crust: Its Composition and Evolution. Blackwell, Oxford, U. K., 312 pp.